Hydration of Cellulose/Silica Hybrids Assessed by Sorption Isotherms

Inês Portugal, Vânia M. Dias, Rui F. Duarte, and Dmitry V. Evtuguin*

Chemistry Department and CICECO, University of Aveiro, Campus de Santiago, 3810-193 Aveiro, Portugal

Received: November 27, 2009; Revised Manuscript Received: February 1, 2010

The hydration of cellulose/silica hybrids (CSH) containing 13, 35, and 46% (w/w) silica synthesized *in situ* by a mild sol−gel aqueous process was studied employing sorption isotherms and surface energy measurements. Water sorption is governed by two simultaneous equilibria at the silica−vapor and cellulose−vapor interfaces due to the presence of cellulose regions covered and uncovered with silica as confirmed by X-ray scattering analysis. The important contribution of a water impermeable cellulose−silica interface to the surface properties of CSH is highlighted. CSH exhibit type II isotherms in the temperature range 15−40 °C, more appropriately described by the Guggenheim−Anderson−de Boer (GAB) model than by the Brunauer−Emmett−Teller (BET) model. Specific surface areas calculated using both models (S_{BET} and S_{GAB}) increase linearly with the amount of silica influencing the higher moisture content of CSH for the same water activity. However, the presence of silica reduces the strength of interaction between monolayer water molecules and the CSH surface as revealed by the net isosteric heat of sorption (35 kJ/mol for cellulosic pulp and 26 kJ/mol for CSH with 35% silica). Silica confers a higher surface energy to CSH contributing to its polar component and surface wettability (contact angle with water) when compared to cellulosic pulp. The average diameter of cellulose microfibrils and the interfacial cellulose−silica areas are assessed on the basis of the analysis of sorption isotherms.

Introduction

Cellulose is the most abundant renewable natural polymer on the Earth. It is composed of β-D-glucopyranosyl units linked by β-(1→4) glucosidic bonds and presents an amorphous-crystalline structure.[1] Due to its unique properties, cellulose is widely demanded in different technical areas and biomedicine.[2] In technical areas, cellulose is used mostly in the form of cellulosic pulp obtained by exhaustive wood delignification and subsequent bleaching.[3] The application domains of cellulose may be substantially expanded if combined with an inorganic phase. The resulting cellulose composites are promising materials compiling in a synergetic way the properties of the starting components.[4,5] Silica derivatives of cellulose are of special interest due to their substantially higher thermal stability, improved lipophilic behavior, and affinity toward specific substrates in comparison to the starting polymer matrix.[4−6] Cellulose/silica hybrids (CSH) are an example of such materials fitting well into the concept of green chemistry, since cellulose is a biodegradable natural polymer. CSH are prepared by a mild sol−gel process at room temperature using cellulosic pulp fibers, tetraethoxysilane (TEOS) as the silica precursor, an acidic catalyst, and a benign solvent such as water or water−ethanol mixtures.[7] The *in situ* generated silica particles are evenly dispersed at the nanometer scale and bound to cellulose through hydrogen or covalent bonds, thus forming a three-dimensional network (Figure 1).[7,8] A major part of silica is deposited as a discontinuous film constituted of round-shape domains of about 30−300 nm and a smaller part in the form of 0.5−3 μm particles.[7,9]

The properties of CSH are significantly different from those of the starting cellulosic material.[7−10] For example, CSH exhibit improved thermal and mechanical stability, dimensional stability upon wetting, excellent heat insulation, and fire resistance properties.[8] Furthermore, the implementation of specific functionalities into CSH expands their field of application.[8,11] The coating of paper with inorganic formulations is another interesting application of cellulose hybrids allowing revolutionary changes in the surface modification toward controlled moisture penetration and printing response (i.e., image transfer capabilities).[9,12] Future applications of CSH require fundamental knowledge of surface properties especially those related to water interactions with the hybrid at the solid−vapor and solid−liquid interfaces. Although this information is available for cellulose and silica, it is still lacking for these new CSH materials. Hence, the main goal of this study was to assess the water sorption patterns on the surface of CSH and to elucidate how the cellulose−silica interface affects these interactions.

Surface characterization tools for fibers and related materials include among others spectroscopic, microscopic, and thermodynamic methods.[13] Spectroscopic and microscopic methods have been employed to provide information about surface chemistry and morphology of CSH.[7−11] The present work focuses on the characterization of surface affinity to water by thermodynamic methods such as sorption isotherms, sorption enthalpies, and contact angle measurements.

Theoretical Basis

Sorption isotherms describe the equilibrium relationship between adsorbate content in the solid material as a function of adsorbate concentration in the gas or liquid phase at constant pressure and temperature. In material science, sorption isotherms are usually measured with nitrogen at 77 K, whereas, in food and cellulose sciences, water sorption isotherms are preferred. The shape of the isotherm depends on the type of adsorbate and adsorbent but also on the molecular interaction between the two phases. The IUPAC classification based on the work of Brunauer et al.[14] includes among others type I isotherms typical of microporous solids (hyperbolic type); type II isotherms typical of finely divided nonporous or macroporous solids and

* Corresponding author. E-mail: dmitrye@ua.pt. Phone: +351-234 401 526. Fax: +351-234 370 084.

10.1021/jp911270y
Published on Web 03/02/2010

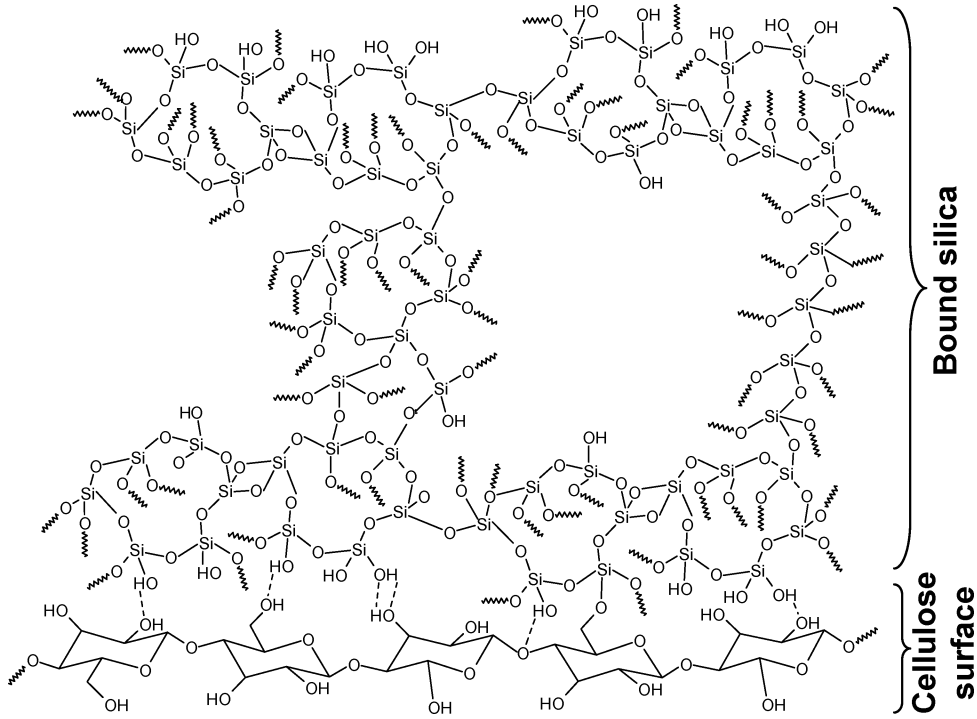

Figure 1. Schematic representation of silica bounded to the cellulosic fiber surface via strong hydrogen bonding in cellulose/silica hybrids. Micropores are formed by four- to eight-membered silica structures, and mesopores appear as cavities between silica domains.

hydrophilic polymers such as natural fibers (S-type); type III isotherms typical of water vapor adsorption on hydrophobic materials such as rubbers, plastics, and synthetic fibers (parabolic type); type IV isotherms of activated charcoal and inorganic materials such as aluminum oxide (similar to type II at low relative pressure); and type V isotherms representative of some mesoporous materials with particularly strong intermolecular interactions (similar to type III at low relative pressure).[14]

Mathematical models suitable to describe adsorption isotherms can be divided into several categories: kinetic models based on multilayer adsorption (Brunauer−Emmett−Teller (BET) equation) or multilayer adsorption and condensed film (Guggenheim−Anderson−de Boer (GAB) equation), semiempirical models (e.g., Henderson and Halsey equations), and empirical models (e.g., Smith and Oswin equations).[15] The BET model represents a fundamental milestone in the interpretation of multilayer sorption isotherms, particularly type II isotherms, but this model is generally restricted to adsorbate low relative pressures ($P/P_0 \leq 0.45$, where P_0 represents the saturation pressure) due to the assumptions used in the derivation of the equation. The GAB model represents an extension of the BET model valid for higher relative pressures ($P/P_0 \leq 0.90$).[16] In this model, a third constant is introduced to describe the modified properties of the sorbate in the multilayer region in relation to the sorbate in the monolayer and in the bulk liquid. Both models may be represented by eq 1:

$$X_{eq} = \frac{X_m C K a_w}{(1 - K a_w)[1 + (C - 1) K a_w]} \quad (1)$$

where X_{eq} is the equilibrium moisture content expressed as grams of adsorbate per gram of adsorbant, a_w is the water activity or more generally the adsorbate relative pressure, X_m, and C and K are the model parameters with $K = 1$ for the BET model and $K \in [0, 1]$ for the GAB model. Theoretically, X_m is the monolayer capacity ($g_{adsorbate}/g_{solid}$) and C and K are adsorption energy parameters with slightly different physical meanings in both models.[14−19] Parameter C is related essentially to differences of sorption enthalpy on the monolayer (H_1) and on the multilayer (H_n), whereas parameter K is related not only to differences between enthalpy in the bulk liquid (H_L) and on the multilayer but to a larger extent to the entropy differences of sorbate molecules. Usually, the maximum enthalpy is reached at the same X_{eq} as the maximum in entropy.[19] The influence of temperature in both parameters is expressed by Arrhenius type equations:

$$C = C_0 \exp\left(\frac{\Delta H_C}{RT}\right) \quad (2)$$

$$K = K_0 \exp\left(\frac{\Delta H_K}{RT}\right) \quad (3)$$

where C_0 and K_0 are entropic accommodation factors, $\Delta H_C = H_1 - H_n$ and $\Delta H_K = H_L - H_n$ are enthalpy differences with H_i defined with reference to the gas phase, R is the ideal gas constant, and T is the absolute temperature.[17,19] Since the BET model assumes $K = 1$ and the same properties for adsorbate molecules in the multilayer and in the liquid bulk, i.e., $H_n = H_L$, for this model, $\Delta H_K = 0$ and $\Delta H_C = H_1 - H_L$. Another difference between the two models is that the BET model assumes complete surface coverage while the GAB model predicts incomplete coverage due to "jamming" of adsorbate molecules at the surface.[17] The fraction of occupied sites in the first layer (ξ^{l_1}) is a function of water activity and the C and K parameters, as defined by eq 4:

$$\xi^{l_1} = \frac{C K a_w}{1 + (C - 1) K a_w} \quad (4)$$

At saturation, $a_w = 1$ and the fraction of occupied sites (ξ^l_{max}) is always lower than 1 because $K \leq 1$.

The specific surface area of a solid (S, $m^2/g_{dry\ solids}$) is related to the monolayer capacity, X_m, by eq 5

$$S = X_m \frac{N_A A_m}{M} \quad (5)$$

where M is the adsorbate molecular weight, N_A the Avogadro number, and A_m the effective cross-sectional area of the adsorbate molecule (0.162 nm^2 for nitrogen at 77 K, 0.125 nm^2 for water at 298 K).[18] Usually, the surface area values obtained with water and nitrogen are quite different due to the chemical nature of water adsorption in comparison with the physical nature of nitrogen adsorption.[18] Moreover, although the influence of temperature on X_m is usually neglected, experimental evidence reveals that X_m decreases significantly with temperature.[19] An exponential type equation similar to eqs 2 and 3 has been proposed, but the equation parameters have no physical meaning.[19]

The total energy required to remove water adsorbed on the adsorbent surface (Q_{st}) is the sum of the latent heat of vaporization of pure water (Q_{vap}) and the net isosteric heat of sorption (Q^{net}_{st}), defined by eqs 6 and 7, respectively:

$$Q_{vap} = 6887 \times R - 5.31 \times RT \quad (6)$$

$$\frac{d(\ln a_w)}{d(1/T)} = \left[-\frac{Q^{net}_{st}}{R}\right]_{Xeq} \quad (7)$$

Q^{net}_{st} is estimated at a specific equilibrium moisture content from sorption isotherms at different temperatures by rewriting the Clausius−Clapeyron equation (7) to obtain water activity as a function of temperature at constant X_{eq} ($\ln a_w = f(1/T)$).[17,19]

Contact angle analysis is based on the wetting of a solid surface with a liquid using either static or dynamic methods.[13] In the static method, a sessile drop of a liquid probe is deposited on the solid surface and the contact angle (θ) is measured. The procedure is repeated for a series of liquid probes and the solid surface free energy (γ_S) and corresponding polar (γ^p_S) and dispersive (γ^d_S) components are obtained from eq 8 and the combined Owens−Wendt−Young equation (9):

$$\gamma_S = \gamma^p_S + \gamma^d_S \quad (8)$$

$$\gamma_L(1 + \cos\theta) = 2\sqrt{\gamma^p_S \gamma^p_L} + 2\sqrt{\gamma^d_S \gamma^d_L} \quad (9)$$

where γ_L, $\gamma_L{}^p$, and $\gamma_L{}^d$ represent the liquid superficial tension and the corresponding polar and dispersive components, respectively.[20]

Materials and Methods

Cellulose/Silica Hybrids. CSH were prepared using *Eucalyptus globulus* bleached kraft pulp (91% ISO brightness, Cacia Pulp mill - SOPORCEL, Portugal) as a cellulosic fiber source. This pulp contained about 14.1% xylan besides cellulose. The silica source was a prehydrolyzed aqueous solution of TEOS (tetraethoxysilan) obtained using HNO_3 as an acidic catalyst (pH 1.2) under vigorous stirring for 40 min at room temperature, until homogeneous solution, and NH_3 as a pH control agent to promote the condensation of silica at a pH around 2.8. The TEOS/H_2O molar ratio was nearly 4. The fibers were disintegrated in water (100 cm^3/g) at room temperature for 24 h, filtered off to low humidity (ca. 50−60%), and added to the previously prepared TEOS solution under vigorous stirring. The TEOS/fiber ratio was around 28. The reaction was allowed to proceed at room temperature (20 °C, pH around 3.0) for the preselected contact time, and the resulting CSH were filtered and dried at 105 °C during a 12 h period. The procedure was repeated using different contact times (2−20 min) to control the amount of silica loaded in the final hybrid material. The percentage of silica in the hybrid was assessed via weight increment of cellulosic pulp after the synthesis. These data are correlated to results obtained by thermogravimetric analysis.[7,8]

Gravimetric Water Sorption. Water sorption isotherms of cellulosic pulp fibers and CSH containing 13, 35, and 46% (w/w) silica were determined by a static-gravimetric method in the range 15−40 °C. Relative humidity was varied in the range 0−100% using different saturated aqueous salt solutions (KOH, CH_3COOK, $MgCl_2 \cdot 6H_2O$, K_2CO_3, $Mg(NO_3)_2$, KI, $(NH_4)_2SO_4$, KNO_3).[21] Cellulose and CSH samples were previously dried at 25 °C under moderate vacuum over P_2O_5 and then placed in net polyester bags that were attached to the top of closed flasks containing the saturated salt solutions. The flasks were placed in a shaking water bath (Julabo SW23) at controlled temperature, and the samples were weighted periodically until reaching equilibrium, i.e., constant weight (approximately 15 days).

Nitrogen Sorption Analysis. Nitrogen adsorption/desorption isotherms of cellulosic pulp and hybrid materials were obtained at 77 K and relative pressures in the range 0.005−0.980 using a Micrometrics Gemini Model 2370 (Norcross, USA). The samples were degassed before analysis (12 h at 100 °C). Forty isotherm points were collected, and the specific surface areas were calculated using the BET equation.

Contact Angle Analysis. Contact angles were measured in a Surface Energy Evaluation System (Advex Instruments) using the sessile drop method and water, formamide (FA), and diiodomethane (DIM) as probe liquids. The solid surface was a nonsized and nonfinished handsheet produced from extractive-free bleached eucalypt kraft pulp (70 g/m^2) without any surface treatment and with the silica sol−gel solution deposited by roll-sizing (about 14 g/m^2) followed by infrared drying for 5 min. The roughness (Bendtsen test according to ISO 8791) of treated and nontreated papers was similar (345 and 355 mL/min, respectively).

Wide Angle X-ray Scattering Analysis (WAXR). Cellulosic pulp and CSH samples were analyzed on a Philips X'Pert MPD diffractometer using a Cu K_α source ($\lambda = 0.154$ nm) in the 2θ range 2−40° and scanning step width of 0.02°/scan. Samples were analyzed as textured analytes using pellets of 12 mm diameter and 1 mm thickness prepared by pressing (50 MPa). For quantitative analysis, the background scattering was subtracted from the pulp diffractogram. The crystalline reflections, amorphous halo, and cellulose degree of crystallinity (DC) were calculated as previously reported.[22]

NMR and Image Analyses. ^{29}Si solid-state magic angle spinning nuclear magnetic resonance (^{29}Si MAS NMR) spectra were recorded on a Bruker Avance 400 spectrometer. Samples were packed into a zirconium rotor sealed with Kel-F caps and spun at 5 kHz. Acquisition parameters were as follows: 90° pulse, contact time 8 ms, pulse delay 60 s. Scanning electron microscopy (SEM) images were obtained on a FEG-SEM

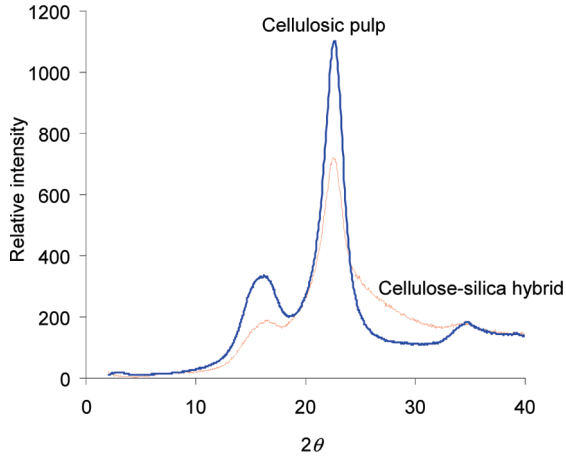

Figure 2. WARX diffractograms of cellulosic pulp and cellulose/silica hybrid containing 35% (w/w) bounded silica.

Hitachi S4100 microscope coupled with an energy dispersive spectrometer (EDS) and operating at 25 kV, using gold coated samples.

Results and Discussion

Accessible Surfaces. The CSH surface possesses a mosaic structure where silica domains are interchanged with cellulosic fiber regions free of silica (Figure 1). The presence of some CSH fibers uncovered with silica was envisaged previously by SEM/EDS (scanning electron microscopy coupled with energy dispersive spectroscopy) and AFM (atomic force microscopy).[7,9] These features were additionally confirmed by WARX studies that revealed cellulose fiber surfaces accessible to X-rays in the CSH materials. Even at relatively high silica content (35% w/w), WAXR diffractograms present well-defined reflections at about 16° (nonresolved reflections from the 101 and 10$\bar{1}$ planes) and at about 22° (reflection from the 002 plane); i.e., the diffraction patterns are consistent with the structure of cellulose I (Figure 2).[1,3] Hence, water interaction with CSH might combine two simultaneously occurring equilibria, i.e., at the silica−vapor and cellulose−vapor interfaces (Figure 3).

The surface of silica comprises essentially SiOH and SiOSi groups (Figures 1 and 3) whose proportions and accessibility to water depend on the particular silica structure.[23,24] The adsorptive character and other surface properties of various silicas have been related to the presence of silanol hydroxyl groups.[23,24] The specific surface area is another factor to consider regarding water sorption capacity. For example, porous silica gels are highly effective desiccants exhibiting specific surface areas up to ca. 200−1500 m^2/g, as determined by nitrogen sorption isotherms.[25−27] The degree of silica cross-linking (η) in CSH (defined as the ratio of effective (f_{ef}) to potential (f_{pot}) functionalities of Si substituted by 1, 2, 3, or 4 OSi moieties, Q_1, Q_2, Q_3, and Q_4 units, respectively) was 0.87−0.88, as determined from ^{29}Si MAS NMR spectra, which is typical for amorphous silica in organic−inorganic hybrids obtained by sol−gel synthesis.[28] This means that roughly each 10th substituent in Si is a hydroxyl group.

Hydroxyl groups are largely responsible for water sorption in cellulose which is a highly hydrophilic material.[3,29−31] However, only 40−60% of the hydroxyl groups are accessible to water because of strong hydrogen bonding between cellulose molecules.[30] Furthermore, the gas sorption capacity of cellulosic materials is limited to the outer surface of individual fibers and is predetermined by the cellulose structural hierarchy.[31] It is

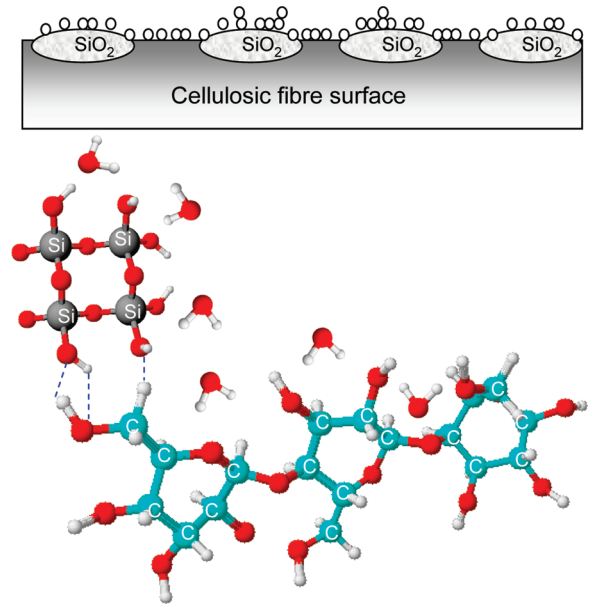

Figure 3. Hydration of the cellulose/silica hybrid surface comprised of interchanged silica domains and uncovered cellulose (top image, the circles depict water molecules). A fragment of the hybrid surface (bottom figure) shows adsorbed water molecules bound to a four-membered silica structure and to cellulose in ball-and-stick representation. The strong hydrogen bonding between silica and cellulose (dashed lines) creates a water impermeable interface.

TABLE 1: Surface Area and Pore Dimensions of Cellulosic Pulp and Cellulose−Silica Hybrids Determined by Nitrogen Adsorption/Desorption Isotherms at 77 K (BET Model)

material	surface area (m^2/g)	average pore width (Å)	total pore volume (mm^3/g)
cellulosic pulp (base material)	1.8	77.9	1.6
CSH, 13% SiO_2	62.6	31.1	26.6
CSH, 35% SiO_2	120.9	27.3	36.1
CSH, 46% SiO_2	157.5	26.0	43.2

well-known that cellulose molecules are organized in elementary fibrils (3.5−4.0 nm width) which are assembled in a twisting mode into microfibrils (15−30 nm width).[1,3] Microfibrils, the main building blocks of plant cell walls, are structurally associated with noncellulosic polysaccharides (hemicelluloses) to a different extent. In the case of eucalyptus cellulosic pulp, microfibrils are bounded to glucuronoxylan (5−18% w/w).[22] According to the "fringed-micelle" theory, the crystalline regions (micelles) alternate with less ordered amorphous regions largely responsible for water sorption.[1,3] In effect, the internal crystalline regions and the external surfaces of elementary fibrils strongly bound in the microfibril assembly are inaccessible to water.[29,32] The drying of cellulosic materials leads to additional aggregation of microfibrils (hornification) drastically decreasing the amount of accessible hydroxyl groups.[33] The degree of crystallinity of the cellulosic pulp used in this study was 71%, as determined by WARX and corrected for the diffraction of noncellulosic components.[22]

The accessible surface in cellulosic pulp and CSH was evaluated via nitrogen sorption/desorption isotherms and the BET approach (Table 1). As could be expected, the progressive incorporation of porous silica into the cellulosic pulp matrix increased significantly the total pore volume and the surface area (S_{BET}) of the hybrid materials. The effect of silica on the hydration of CSH has been evaluated by analysis of the water sorption isotherms.

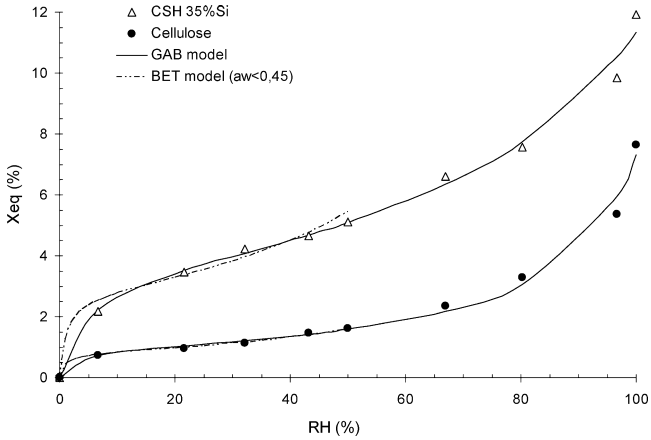

Figure 4. Water adsorption isotherms for cellulose and CSH (35% SiO_2) at 30 °C. Experimental data (points) and curve fitting with BET and GAB model equations.

Water Sorption Isotherms. Experimental data for water adsorption by cellulose and CSH (35% silica) at 30 °C, presented in Figure 4 as an example, are consistent with type II isotherms usually associated with hydrophilic polymers such as cellulose.[3,29,31] Silica usually presents type I (micro- and mesoporous silica) or types IV/V (wide-pore silica) sorption isotherms.[25] The type II isotherm observed for CSH indicates that cellulose governs the hybrid sorption behavior. The equilibrium moisture content (X_{eq}) increases with water activity (a_w) and is significantly higher for CSH when compared to cellulose. Several isotherm equations were fitted to the experimental data by nonlinear regression and compared by means of statistical analysis. Despite satisfactory fitting to the experimental data, empirical and semiempirical models such as the Henderson model were discarded for further analysis because of a lack of physical meaning of the model parameters. The GAB model was identified as suitable over the entire range of water activity. The BET model although appropriate only for low water activities ($a_w \leq 0.45$) was selected as a reference, since it is recommended by IUPAC for the surface characterization of porous materials. The BET and GAB parameters (X_m, C, and K) for water adsorption on cellulose and CSH with different silica contents are presented in Table 2. Specific surface areas (S) obtained from water sorption isotherms were calculated according to eq 5.

X_m values, and consequently S values, are systematically lower for the BET model (Table 2). This behavior was previously highlighted by Timmermann[16] and relates to the limited range of water activity for which the BET model holds in comparison with the broader range of applicability and the additional parameter of the GAB model. The physical differences between the two models were revealed by Pradas et al. through the thermodynamic derivation of the BET and GAB equations.[17] It was suggested that the GAB model implies an incomplete occupation of the monolayer even at saturation due to "jamming" of molecules on the adsorbent's surface; i.e., the model accounts for sorbate−sorbate molecular interactions. This phenomenon that complies with Monte Carlo simulations and is not predicted by the BET model could explain the systematic differences for X_m obtained with both models. In fact, the discrepancies between S_{BET} and S_{GAB} are higher for CSH when compared to cellulosic pulp and this can be related to the lower number of occupied sites in the hybrid materials. For instance, for CSH with 46% silica, the occupied sites reach 90% at a_w = 0.35 and 98.4% upon saturation, whereas cellulose occupation reaches 90% at a_w = 0.15 and 99.6% upon saturation (ξ^{l}_{max}, Table 2).

TABLE 2: BET and GAB Model Parameters for Cellulose and CSH Materials with Different Silica Contents (Water Adsorption at 303 K)

			cellulose/silica hybrids		
model	parameters	cellulose	13% SiO_2	35% SiO_2	46% SiO_2
GAB	C	53.5	51.6	35.2	36.6
	K	0.823	0.767	0.617	0.633
	X_m	0.015	0.022	0.047	0.057
	E^a (%)	4.3	7.4	6.1	7.2
	S (m^2/g)	62	90	195	237
	$S_0{}^b$ (m^2/g)		117	210	256
	ξ^{l}_{max} (%)	99.6	99.4	98.3	98.4
BET, $a_w \leq 0.45$	C	115.8	114.6	105.1	83.5
	X_m	0.01344	0.01956	0.03732	0.04602
	E^a (%)	4.1	9.2	7.8	9.8
	S (m^2/g)	56	82	156	192

[a] $E = (1/n)\sum_{i=1}^{n}(|X_{eq_i} - X^{calc}_{eq_i}|/X_{eq_i}) \times 100$, where X_{eq_i} is the observed moisture content, $X^{calc}_{eq_i}$ is the moisture content predicted by the model, and n is the number of observations. For practical purposes, a mean relative deviation modulus below 10% is indicative of a reasonable good fit. [b] $S_0 = W_{cell} \times S_{cell} + W_{Si} \times S_{Si}$, where W_{cell} and W_{Si} are the weight fractions of cellulosic pulp and silica, respectively, in hybrids and S_{cell} and S_{Si} are the specific surfaces (m^2/g) of cellulosic pulp and silica, respectively. S_{Si} was estimated by extrapolating S data for CSH to zero cellulose content (483 m^2/g).

TABLE 3: Surface Energies of Cellulosic Pulp Handsheets Uncovered and Covered with CSH

	contact angle (θ) (deg)			surface energy (mJ/m^2)		
material	water	FA	DIM	γ^d_S	γ^p_S	γ_S
pulp	78.5	48.8	44.5	34.5	5.4	39.4
coated pulp[a]	65.9	28.5	45.1	32.2	12.6	44.8

[a] Silica content about 28%.

The values of X_m increase linearly with CSH silica content due to the higher number of specific surface sites available for water sorption (Table 2). Similar features were observed earlier for moisture sorption on silicified microcrystalline cellulose (SiMCC)[34] and nitrogen sorption on siliceous lignins.[35] Simultaneously, the importance of silica interaction with cellulose during the hydration of CSH should be highlighted as revealed from the results presented in Table 3 for silica coated paper produced from the same cellulosic fibers as CSH. Silica coated paper showed a small increase of surface wettability when compared to the uncoated paper (contact angles 65.9 and 78.5°, respectively), whereas the total surface energy, particularly its polar component, increased significantly (Table 3). This apparent controversy can be explained by the interaction of cellulose and silica in CSH via strong hydrogen bonding of hydroxyl groups, first with preformed soluble silica oligomers and then with bulk silica after curing (Figures 1 and 3). Consequently, the cellulose−silica interface impedes water penetration inside the fibers though the free polar sites of silica on the paper surface remain accessible. Apparently, the surface energy is particularly sensitive to the thin silica layer deposited on the surface of fibers and much less sensitive to the amount of silica loaded inside the fibers, although this affects the wettability of the hybrid material. The accessible areas of CSH (S) are lower than those theoretically predicted (S_0) neglecting the interfacial interactions and assuming a physical mixture of cellulosic pulp and silica in CSH (Table 2). The interfacial surface areas (S_{if}) estimated with eq 10

$$S_{if} = (S_0 - S)/2 \quad (10)$$

varied between 7.5 and 13.5 m^2/g for CSH. Strong binding between cellulose and silica and the formation of a water impermeable "glassy" interface explains the previously observed 10 times lower water retention values of CSH in comparison with cellulosic pulp.[8]

Water sorption by silica and cellulose proceeds via similar mechanisms.[31] However, the porous structure of silica is rigid and stable, whereas cellulose presents a nonrigid structure influenced by the presence of sorbate vapors and their thermodynamic properties. Water interaction with cellulose increases the accessible areas, via cleavage of intermolecular hydrogen bonds, promoting fiber swelling and increasing "internal" water content. Unlike cellulose, the accessible area of silica pores maintains the same contribution to the "external" water content of hybrid materials. Kachirimanis et al. commented on this behavior by quantifying the "internal" and "external" moisture content that clearly revealed a higher capacity of SiMCC for "external" adsorption especially in the range of high water activity.[34]

The values of specific surface areas presented in Tables 1 and 2 for cellulose and CSH were obtained from nitrogen and water sorption isotherms using the BET model. Surface areas increase linearly with silica content for both adsorbates, but the values obtained from water sorption isotherms are systematically higher than those obtained from nitrogen sorption data. For CSH, the results differ 20−30%, whereas, for cellulose, the differences are remarkably higher: 1.8 and 56 m^2/g from N_2 and water sorption data, respectively. This behavior has been observed for MCC with differences of 2 orders of magnitude (e.g., for MCC 101, the reported surface areas are 1.04 and 124 m^2/g from N_2 and water sorption data, respectively).[36] This difference was assigned to the accessibility of water molecules within the interstices of cellulose fibers which promotes swelling, while nitrogen adsorbs only on the external surface of the fibril aggregates without the swelling effect.[36] The difference in surface areas accessible to nitrogen and water are not so remarkable for CSH as for cellulose because even if silica favors the attraction of water molecules, due to its high surface area and polarity, the strong silica binding with cellulose reduces the swelling effect. This is the reason for the significantly higher dimensional stability of CSH upon humidification in contrast to cellulosic pulp.[8]

Specific surface area provides knowledge on the effective width of microfibrils based on their accessibility toward water vapor. This information may be useful to assess the fibril aggregation. Assuming microfibrils as rods with a round cross section, the relation between S and the average diameter (D) of a microfibril may be expressed by eq 11

$$S\,(m^2/g) = \frac{A}{m} = \frac{\pi DL}{\rho_{cell} V} = \frac{4}{D\rho_{cell}} \quad (11)$$

where m, L, A, and V are the weight, the length, the surface area, and the volume of the microfibril, respectively. The cellulose density (ρ_{cell}) was evaluated as 1.54×10^6 g/m^3 using eq 12

$$\rho_{cell} = DC \times \rho_{cr} + (1 - DC) \times \rho_a \quad (12)$$

where DC is the degree of crystallinity (71% or DC = 0.71) and ρ_{cr} and ρ_a are the specific weights of crystalline and amorphous cellulose, respectively ($\rho_{cr} = 1.59$ g/cm^3 and $\rho_a = 1.40$ g/cm^3).[37,38] The average diameter of cellulose microfibrils—25.0 nm, obtained from data at 25 °C ($S = 104$ m^2/g, Table 4)—is very close to the values previously determined by AFM (15−25 nm)[9] and solid state ^{13}C NMR (ca. 20 nm)[22] for eucalyptus kraft pulp cellulose. The increase in temperature from 25 to 30 °C almost duplicates the effective width of microfibrils (from 25.0 to 41.9 nm), indicating their possible aggregation due to elimination of bound water and the restoring of interfibrillar hydrogen bonds. Obviously, during the CSH synthesis, certain portions of the liquid silica formulation, whose oligomers possess a gyration radius ≪2 nm, penetrate the interfibrillar space (2−6 nm).[3] Hence, the fibril areas that are in touch with the formulation will be inaccessible for water after the formation of the silica network during curing. It may be proposed that the silica network formed during CSH synthesis covers preferentially the amorphous regions of cellulose, which are the most accessible not only for water adsorption but also for the silica formulation. The crucial role of accessible hydroxyl groups on the fiber surface for the silica uptake was discussed previously.[8] Silica oligomers bound to cellulose are the nucleation centers for the growing silica network assembled via self-condensation reactions with other silica oligomers. Therefore, the cellulose fibrils embedded into the silica matrix possess a lower activity and surface area toward water sorption than the original fibrils. For example, if a similar aggregation of microfibrils in cellulose is assumed for the cellulosic pulp and for the hybrids, the partial contribution of cellulose area accessible to water (S^p_{cell}, m^2/g) decreases almost 50% for CSH with 35% SiO_2 when compared to parent cellulosic pulp (from

TABLE 4: GAB Model Parameters for Water Adsorption on Cellulose and CSH in the Range 15−40 °C

		temperature (°C)						
	parameters	15	20	25	30	35	40	ΔH_i (kJ/mol)
CSH, 35% SiO_2	C	48.2	42.5	38.2	35.2	31.4	26.0	$\Delta H_C = 17$
	K	0.54	0.57	0.58	0.62	0.69	0.74	$\Delta H_K = -9$
	X_m	0.078	0.067	0.058	0.047	0.035	0.027	
	E^a (%)	4.1	5.2	5.3	6.1	2.6	4.3	
	S (m^2/g)	323	277	240	195	147	111	
	$\xi^{l_1}_{max}$ (%)	98.3	98.3	98.1	98.3	98.6	98.7	
cellulose	C			65.0	53.5	47.4		$\Delta H_C = 24$
	K			0.76	0.82	0.87		$\Delta H_K = -11$
	X_m			0.025	0.015	0.009		
	E^a (%)			3.7	4.3	4.7		
	S (m^2/g)			104	62	38		
	$\xi^{l_1}_{max}$ (%)			99.5	99.6	99.7		

[a] Mean deviation modulus, as defined in Table 2.

62 in pulp to 33 m^2/g in CSH at 30 °C). S^p_{cell} was calculated from eq 13:

$$S^p_{cell} = S_{cell} W_{cell} - S_{if} \quad (13)$$

where S_{if} is the inaccessible interface surface (eq 10) and S_{cell} and W_{cell} are the cellulose surface area (62 m^2/g) and the weight fraction (0.65), respectively, in CSH with 35% silica (Table 2).

Water Sorption Thermodynamics. The parameters C (BET and GAB models) and K (GAB model) are energetic parameters related to the heat of adsorption on the monolayer and on the upper layers, respectively.[15−17,19] The value of the C parameter for cellulose is higher than that for the hybrid materials and indicates a stronger interaction between the solid surface and water in the monolayer (Table 2). The presence of a silica network covering the cellulose fibers increases the total surface area of CSH, as discussed previously, but reduces drastically the values of C because this network diminishes the number of cellulose accessible OH groups. The reduction of bound water due to the introduction of silica into cellulose is well documented.[7,8,10,11]

The K parameter (GAB model) decreases in the presence of silica but remains in the range 0.6−0.8, demonstrating the existence of a structured multilayer with properties distinct from the bulk liquid (Table 2). Recalling that K is related predominantly to the enthalpy of the sorbate in the structured multilayer, its decrease in the series of CSH with increasing silica content may be interpreted as enhancement of the spatial order of the water molecules in the multilayer of the hybrid materials. This is in agreement with experimental data and model simulations for water interaction with silica, namely, water aggregation in clusters in boundary layers.[24,39,40] The thermodynamic parameters of these interactions were further discussed analyzing the water sorption isotherms of cellulose and CSH obtained at different temperatures (Figure 5).

The temperature dependence of GAB parameters C and K together with the enthalpy differences ΔH_C and ΔH_K calculated by linearization of eqs 2 and 3 are presented in Table 4. As can be seen for cellulosic pulp and CSH containing 35% silica, temperature has a positive effect on K and a negative effect on C. This behavior has been reported previously for starch, a polymer structurally similar to cellulose.[19,41] Recalling the definitions of $\Delta H_C = H_1 - H_n$ and $\Delta H_K = H_L - H_n$, it may be concluded that the enthalpy associated with adsorbed water molecules follows the order $H_1 > H_n > H_L$ and thus corroborates the aforementioned stronger interactions of water molecules in the monolayer in comparison with the multilayer.

The ΔH_C values reveal a higher difference in energies between molecules in the monolayer and in the multilayer for cellulose than for CSH (Table 4). Hence, the presence of silica weakens the interaction between the surface and the monolayer water molecules. Since $|\Delta H_K|$ is also higher for cellulosic pulp, the net isosteric heat of sorption, defined theoretically as $Q^{net}_{st} = \Delta H_C + (-\Delta H_K)$, is substantially higher for cellulosic pulp in comparison to CSH (35 and 26 kJ/mol, respectively). Therefore, the incorporation of silica into cellulose weakens the interactions of water with the surface and diminishes the entropy of sorbate molecules in the multilayer. These statements are additionally supported by the results obtained for the total heat of sorption (Q_{st}) of water vapor as a function of moisture content (X_{eq}).

The heat of sorption curve (Figure 6) of the studied materials goes through a maximum at relatively low water content (<5%)

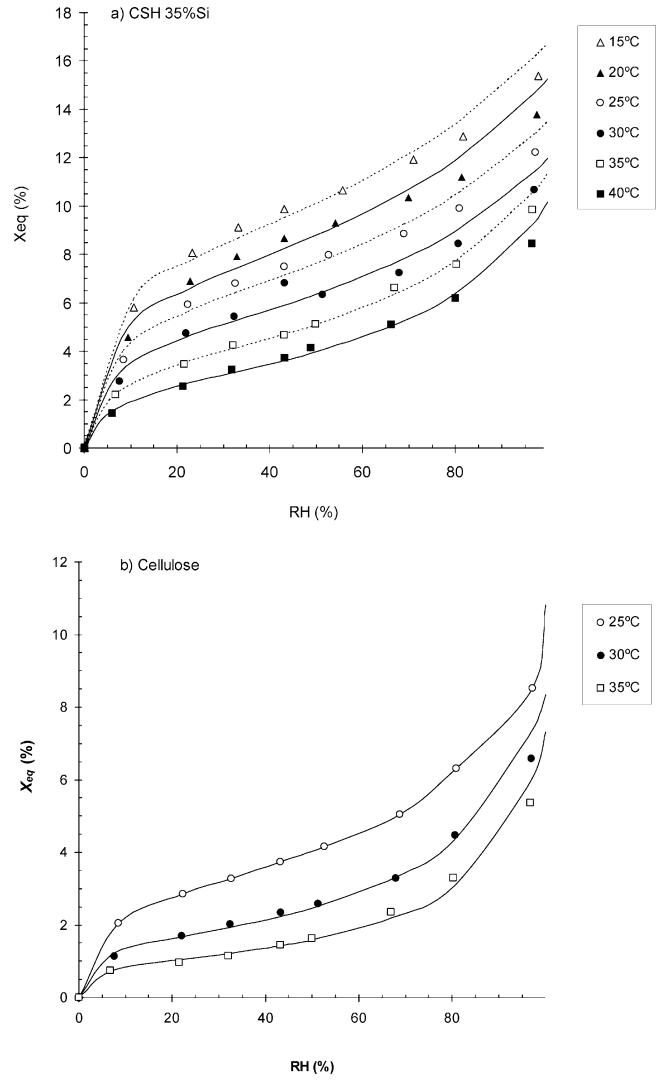

Figure 5. Experimental data and GAB model fitting (curves) for water adsorption isotherms at different temperatures: (a) CSH with 35% SiO_2; (b) cellulose.

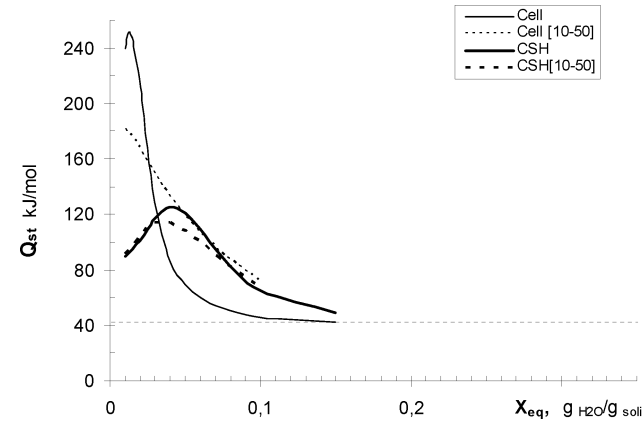

Figure 6. Heat of sorption as a function of moisture content for cellulose and CSH (35% SiO_2). Solid lines represent calculations performed within the range of experimental data. Dashed lines represent calculations performed by extrapolation of eqs 2 and 3 in the range 10−50 °C. The horizontal line represents the heat of vaporization of pure water at an average temperature.

and then drops until the heat of sorption equals the heat of evaporation of pure water, i.e., the region where the adsorbed water may be considered as "free water" with properties similar

to those of the bulk liquid. Usually, the high values of the Q_{st} maximum at low moisture content are associated with strong attraction forces between active sorption sites and sorbate molecules in the monolayer, whereas lower values of the Q_{st} maximum at relatively high moisture content are associated with weaker interactions in the monolayer.[19] Even though the adequacy of the isotherm model equations in the region of low water activity is doubtful, Ruckold et al. concluded that beyond the Q_{st} maximum the results obtained from water sorption data are consistent with the results from thermal analysis.[42] In this context, comparison of results beyond the Q_{st} maximum is meaningful and the differences between the behavior of cellulosic pulp and CSH under humidification are reliable. Therefore, the significantly higher heat of sorption of cellulose in the region of low moisture content (<2%) and the lower heat of sorption in the region above 3% moisture (Figure 6) might be related to stronger monolayer interactions and weaker multilayer interactions for cellulose when compared to CSH in agreement with the previous discussion. The occurrence of a maximum in the Q_{st} curve has been previously observed for starch and attributed to the existence of sorption sites with different activity and to preferential occupation of the most active sites at low water content.[19,43] In cellulose, these higher activity sites occur predominantly in the amorphous regions of elementary fibrils and most probably are 3-hydroxyl and 6-hydroxyl or 2-hydroxyl and 6-hydroxyl groups of neighboring glucopyranose residues.[29]

The Q_{st} values obtained for cellulosic pulp and CSH are of the same order of magnitude as those for chemisorption (Figure 6). This curious fact may be explained by the nonquantitative nature of the Q_{st} values obtained by linearization of the Clausius−Clapeyron equation (7) assuming that Q_{vap} and Q_{st}^{net} are invariant with temperature. Additional inaccuracies emerge from experimental and graphical errors. Moreover, the calculations of Q_{st} were performed using experimental data from a narrow temperature range (15−40 °C for CSH and 25−35 °C for cellulose). When these calculations were repeated in a wider range of temperature (10−50 °C) by extrapolation of eqs 2 and 3, the Q_{st} maxima decreased notably (curves are designated as CSH[10-50] and Cell[10-50] in Figure 6). These recalculations clearly point out that the assessment of isosteric heat of sorption requires rigorous experimental data from a set of isotherms obtained over a wide range of temperatures. Furthermore, the experimental procedure and calculations should be carefully planed to reduce the uncertainty associated with the parameters of eqs 2 and 3.[43] Qualitatively, the heat of sorption results reveal undeniably significant differences between cellulose and CSH. More accurate results ought to be obtained by calorimetric analysis which is more reliable than the analysis by sorption isotherms at different temperatures.

Nevertheless, it seems that the net isosteric heat of sorption of cellulosic pulp and CSH calculated by the theoretical approach ($Q_{st}^{net} = \Delta H_C + (-\Delta H_K)$) reflect adequately the enthalpy of water sorption. In fact, the value obtained for cellulose (35 kJ/mol) is comparable to the values obtained for starch, a polymer structurally similar to cellulose, by the same approach (17−40 kJ/mol)[19,41] and to those obtained for softwood cellulosic pulps by modulated differential scanning calorimetry (19−23 kJ/mol).[44] It should be noted that the presence of remarkable amounts of concomitant xylan in eucalyptus cellulosic pulps might explain the higher Q_{st}^{net} values in comparison to softwood pulps. Xylan is located essentially on the surface of microfibrils,[1,3] and its integral heat of wetting (130 J/g)[45] almost triples that of cellulose (40−50 J/g).[46,47] Since the integral heat of wetting describes the same sorption phenomena as Q_{st}^{net},[48] the presence of xylan might contribute to the increase of Q_{st}^{net} of cellulosic pulp fibers.

Since the net isosteric heat of sorption of cellulosic pulp (35 kJ/mol) is similar to those reported for silicas of different porosity (39−47 kJ/mol),[25] the significant difference between the heat of sorption of cellulosic pulp and CSH (Figure 6) may be explained by the formation of a cellulose−silica interface during the hybrid synthesis that provides rather particular sorption properties to CSH materials.

Conclusions

Sorption isotherms were used to study the hydration of cellulose/silica hybrids (CSH) containing 13−46% silica, prepared from cellulosic eucalypt pulp and tetraethoxysilane by a mild sol−gel process. This study allowed several major conclusions which may be formulated as follows:

(i) Water sorption by cellulosic pulp and CSH followed type II isotherms. CSH sorption isotherms are described better by the GAB model ($a_w \leq 0.96$) than by the BET model ($a_w \leq 0.45$), although for cellulosic pulp both models showed equally good correlations. This is related to the important contribution of sorbate−sorbate interactions in the multilayer which are considered by the GAB model through the introduction of the thermodynamic parameter K.

(ii) In the temperature range 15−40 °C, at the same water activity, the equilibrium moisture content (X_{eq}) is significantly higher for CSH than for cellulose. This fact is assigned to the higher specific area of CSH (up to 4 times higher than for the cellulosic pulp) which increased linearly with the amount of silica. Simultaneously, the heat of sorption for CSH with 35% SiO_2 is almost half of that found for cellulosic pulp. This is caused by weaker interactions of monolayer water molecules with the CSH surface than with the cellulosic pulp surface. The net isosteric heat of sorption for cellulosic pulp and CSH with 35% silica was of 35 and 26 kJ/mol, respectively.

(iii) The presence of silica confers a higher surface energy to CSH materials due to an increment of the polar component and wettability (higher contact angle with water) when compared to cellulosic pulp. A new approach based on the analysis of sorption isotherms has been proposed to assess this interfacial area and the average diameter of cellulose microfibrils.

Acknowledgment. This study was financially supported by "Agência de Inovação" (grant QREN n° 5348) and by Research Institute on Forestry and Paper (RAIZ, Portugal).

Supporting Information Available: Table showing water activity (a_w) in the atmosphere of saturated aqueous salts as a function of temperature (K); figures showing a ^{29}Si MAS NMR spectrum of CSH (Figure A) and SEM images and EDS data of cellulosic pulp and CSH (Figures B and C, respectively). This material is available free of charge via the Internet at http://pubs.acs.org.

References and Notes

(1) O'Sullivan, A. C. *Cellulose* **1997**, *4*, 173–207.
(2) Klemm, D.; Heublein, B.; Fink, H. P.; Bohn, A. *Angew. Chem., Int. Ed. Engl.* **2005**, *44*, 3358–3393.
(3) Fengel, D.; Wegener, G. *Wood. Chemistry, Ultrastructure, Reactions*; Walter de Gruyter: Berlin, 1984.
(4) Petzold, K.; Koschella, A.; Klemm, D.; Heublein, B. *Cellulose* **2003**, *10*, 251–269.
(5) Gill, R. S.; Marques, M.; Larsen, G. *Microporous Mesoporous Mater.* **2005**, *85*, 129–135.

(6) Heinze, T.; Liebert, T. *Prog. Polym. Sci.* **2001**, *26*, 1689–1762.
(7) Sequeira, S.; Evtuguin, D. V.; Portugal, I.; Esculcas, A. P. *Mater. Sci. Eng., C* **2007**, *27*, 172–179.
(8) Sequeira, S.; Evtuguin, D. V.; Portugal, I. *Polym. Compos.* **2009**, *30*, 1275–1282.
(9) Paiva, A. T.; Sequeira, S.; Evtuguin, D. V.; Kholkin, A. L.; Portugal, I. In *Modern Research and Educational Topics in Microscopy*; Méndez-Vilas, A., Díaz, J., Eds.; FORMATEX: Badajoz, Spain, 2007; Vol. 2, pp 726−733.
(10) Barud, H. S.; Assuncão, R. M. N.; Martines, M. A. U.; Dexpert-Ghys, J.; Marques, R. F. C.; Messaddeq, Y.; Ribeiro, S. J. L. *J. Sol.-Gel Sci. Technol.* **2008**, *46*, 363–367.
(11) Hou, A. Q.; Shi, Y. Q.; Yu, Y. H. *Carbohydr. Polym.* **2009**, *77*, 201–205.
(12) Yoldas, B. E. *J. Sol-Gel Sci. Technol.* **1998**, *13*, 147–152.
(13) Merrett, K.; Cornelius, R. M.; McClung, W. G.; Unsworth, L. D.; Sheardown, H. *J. Biomater. Sci., Polym. Ed.* **2002**, *13*, 593–621.
(14) Brunauer, S.; Deming, L. S.; Deming, W. S.; Teller, E. *J. Am. Chem. Soc.* **1940**, *62*, 1723–1732.
(15) Al-Muhtaseb, A. H.; McMinn, W. A. M.; Magee, T. R. A. *Food Bioprod. Process.* **2002**, *80*, 118–128.
(16) Timmermann, E. O. *Colloids Surf., A* **2003**, *220*, 235–260.
(17) Pradas, M. M.; Sanchez, M. S.; Ferrer, G. G.; Ribelles, J. L. G. *J. Chem. Phys.* **2004**, *121*, 8524–8531.
(18) Robens, E.; Dabrowski, A.; Kutarov, V. V. *J. Therm. Anal. Calorim.* **2004**, *76*, 647–657.
(19) Quirijns, E. J.; van Boxtel, A. J. B.; van Loon, W. K. P.; van Straten, G. *J. Sci. Food Agric.* **2005**, *85*, 1805–1814.
(20) Owens, D. K.; Wendt, R. C. *J. Appl. Polym. Sci.* **1969**, *13*, 1741–1747.
(21) Greenspan, L. *J. Res. Natl. Bur. Stand.* **1977**, *81*, 89–96.
(22) Rebuzzi, F.; Evtuguin, D. V. *Macromol. Symp.* **2006**, *232*, 121–128.
(23) Bhambhani, M. R.; Cutting, P. A.; Sing, K. S. W.; Turk, D. H. *J. Colloid Interface Sci.* **1972**, *38*, 109–117.
(24) Zhuravlev, L. T. *Colloids Surf., A* **2000**, *173*, 1–38.
(25) Rojas, F. J.; Hines, A. L.; Pedram, E. *Ind. Eng. Chem. Process Des. Dev.* **1982**, *21*, 760–764.
(26) Ng, K. C.; Chua, H. T.; Chung, C. Y.; Loke, C. H.; Kashiwagi, T.; Akisawa, A.; Saha, B. B. *Appl. Therm. Eng.* **2001**, *21*, 1631–1642.
(27) Kondrashova, N. B.; Vasil'eva, O. G.; Val'tsifer, V. A.; Astaf'eva, S. A.; Strel'nikov, V. N. *Russ. J. Appl. Chem.* **2009**, *82*, 1–5.
(28) Fidalgo, A.; Nunes, T. G.; Ilharco, L. M. *J. Sol.-Gel Sci. Technol.* **2000**, *19*, 403–407.
(29) Pizzi, A.; Bariska, M.; Eaton, N. J. *Wood Sci. Technol.* **1987**, *21*, 317–327.
(30) Evtuguin, D. V.; Ivanova, T. *Izv. St. Petersburg Forest Technical Acad.* **1995**, *3* (161), 97–104.
(31) Chirkova, J.; Andersons, B.; Andersone, I. *J. Colloid Interface Sci.* **2004**, *276*, 284–289.
(32) Hult, E. L.; Larsson, P. T.; Iversen, T. *Polymer* **2001**, *42*, 3309–3314.
(33) Newman, R. H. *Cellulose* **2004**, *11*, 45–52.
(34) Kachrimanis, K.; Noisternig, M. F.; Griesser, U. J.; Malamataris, S. *Eur. J. Pharm. Biopharm.* **2006**, *64*, 307–315.
(35) Telysheva, G.; Dizhbite, T.; Evtuguin, D. V.; Mironova-Ulmane, N.; Lebedeva, G.; Andersone, A.; Bikovens, O.; Chirkova, J.; Belkova, L. *Scripta Mater.* **2009**, *60*, 687–690.
(36) Kocherbitov, V.; Ulvenlund, S.; Kober, M.; Jarring, K.; Arnebrant, T. *J. Phys. Chem. B* **2008**, *112* (12), 3728–3734.
(37) Sugiyama, J.; Vuong, V.; Chanzy, H. *Macromolecules* **1991**, *24*, 4168–4175.
(38) Chen, W.; Lickfield, G. C.; Yang, C. Q. *Polymer* **2004**, *45*, 1063–1071.
(39) Du, M. H.; Wang, L. L.; Kolchin, A.; Cheng, H. P. *Eur. Phys. J. D* **2003**, *24*, 323–326.
(40) Burneau, A.; Barres, O.; Gallas, J. P.; Lavalley, J. C. *Langmuir* **1990**, *6*, 1364–1372.
(41) Al-Muhtaseb, A. H.; McMinn, W. A. M.; Magee, T. R. A. *J. Food Eng.* **2004**, *62*, 135–142.
(42) Ruckold, S.; Isengard, H. D.; Hanss, J.; Grobecker, K. H. *Food Chem.* **2003**, *82*, 51–59.
(43) Quirijns, E. J.; van Boxtel, A. J. B.; van Loon, W. K. P.; van Straten, G. *J. Sci. Food Agric.* **2005**, *85*, 175–185.
(44) Park, S.; Venditti, R. A.; Jameel, H.; Pawlak, J. J. *Cellulose* **2007**, *14*, 195–204.
(45) Dudkin, M. S. *Russ. Chem. Rev.* **1962**, *31*, 549–556.
(46) Irklei, V. M.; Starunskaya, T. P.; Bychkovskii, N. I.; Kolpakova, I. D.; Nosov, M. P. *Fibre Chem.* **1984**, *15*, 274–276.
(47) Varga, K.; Schadel, U.; Nilsson, H.; Persson, O.; Schuster, K. C. *Fibres Text. East. Eur.* **2007**, *15*, 59–63.
(48) Morrison, J. L.; Dzieciuch, M. A. *Can. J. Chem.* **1959**, *37*, 1379–1390.

JP911270Y